PHYSICAL REVIEW B **71**, 081304(R) (2005)

Evolution of the bilayer $\nu=1$ quantum Hall state under charge imbalance

W. R. Clarke,[1,*] A. P. Micolich,[1] A. R. Hamilton,[1] M. Y. Simmons,[1] C. B. Hanna,[2] J. R. Rodriguez,[2] M. Pepper,[3] and D. A. Ritchie[3]

[1]*School of Physics, University of New South Wales, Sydney, New South Wales 2052, Australia*

[2]*Department of Physics, Boise State University, Boise, Idaho 83725-1570, USA*

[3]*Cavendish Laboratory, University of Cambridge, Cambridge CB3 0HE, United Kingdom*

(Received 23 November 2004; published 10 February 2005)

We use high-mobility bilayer hole systems with negligible tunneling to examine how the bilayer $\nu=1$ quantum Hall state evolves as charge is transferred from one layer to the other at constant total density. We map bilayer $\nu=1$ state stability versus imbalance for five total densities spanning the range from strongly interlayer coherent to incoherent. We observe competition between single-layer correlations and interlayer coherence. Most significantly, we find that bilayer systems that are incoherent at balance can develop spontaneous interlayer coherence with imbalance, in agreement with recent theoretical predictions.

DOI: 10.1103/PhysRevB.71.081304 PACS number(s): 73.43.−f, 73.21.−b

The integer[1] and fractional[2] quantum Hall (QH) effects highlight the role of quantization and interactions in two-dimensional (2D) electron systems. Bilayer systems consist of two parallel, closely spaced 2D electron layers separated by an insulating barrier, with a total carrier density $n_T=n_t+n_b$ where n_t and n_b are the carrier densities of the top and bottom layers, respectively. Bilayer QH states, analogous to those in single 2D layers, are observed at integer and fractional total filling factors $\nu=hn_T/eB$ $(=\nu_t+\nu_b)$, where B is the applied perpendicular magnetic field.[3,4] These bilayer QH states can be attributed to one or more of three mechanisms: (i) the addition of two independent single-layer QH states at even integer bilayer filling factors,[5] (ii) the symmetric-antisymmetric gap Δ_{SAS} established by interlayer tunneling at odd integer bilayer filling factors;[5] and (iii) spontaneous interlayer coherence (SILC), which produces remarkable bilayer QH states with no counterpart in single-component systems.[3–5]

The bilayer $\nu=1$ SILC QH state, hereafter referred to as the SILC state, results from correlations between electrons in different layers that unify the two layers into a single system when the layer separation is sufficiently small.[4] The relative strength of the interlayer and intralayer interactions governs the existence of the SILC state, and is parametrized by the ratio d/l_B, where d is the layer separation and $l_B=(\hbar/eB)^{1/2}=(2\ \ n_T)^{-1/2}$ is the magnetic length at $\nu=1$. Using front and back gates, it is possible to alter n_T, and hence d/l_B, electrostatically. Significant attention is currently focused on understanding how the SILC state evolves as the electron densities in the two layers are unbalanced at constant n_T (i.e., constant d/l_B) by transferring charge from one layer to the other—a process known as charge imbalance. A key question is: for $d/l_B>1.8$, where the SILC state is not observed at equal layer densities can charge imbalance be used to induce a SILC state? Our results indicate that the answer is yes.

In this Communication, we map the existence and stability of the SILC state as the layer densities are unbalanced at constant n_T, spanning the entire range from balanced to completely imbalanced (all charge in one layer). We repeat this process for five densities $(0.82<n_T<1.8)\times10^{11}$ cm^{-2}, ranging from strongly interlayer coherent $(d/l_B=1.26)$ to incoherent at balance $(d/l_B=1.82)$. Our mapping of the stability of the SILC state versus d/l_B and imbalance exhibits diverse behaviors, and we emphasize three key results. First, we identify the point at which the bilayer system undergoes total charge transfer (all the charge in a single layer) and note that it is significantly enhanced by exchange-correlation effects. Second, we observe direct competition between the SILC state and the single-layer QH states in weakly coherent systems. Finally, our third and most significant result is that a bilayer system that is incoherent at balance can develop SILC as the layers are imbalanced.

The continuous evolution of the SILC state into the single-layer $\nu=1$ QH state with charge imbalance was established by Hamilton *et al.*[6] Several authors have since studied this evolution, focusing on the stability of the SILC state, as measured by the width of the quantum Hall plateau[7] or the activation gap $\Delta_{\nu=1}$.[8,9] However, those studies were either complicated by the presence of a tunneling gap that was significantly larger than the $\nu=1$ transport gap ($\Delta_{SAS}=6.8$ K in Ref. 7 and 15 K in Ref. 8) or restricted to a limited range of imbalance.[9] Hence a comprehensive study of the imbalanced $\nu=1$ SILC state without the tunneling contribution has not been achieved until now.

Recent Hartree-Fock calculations have predicted two interesting properties of bilayer systems when imbalanced. First, the $\nu=1$ SILC state is not destroyed by charge imbalance, as might naively be expected.[10] Instead, the excitation gap remains constant until all the charge has been transferred into a single layer.[11] Second, and more significantly, these calculations suggest that imbalance should stabilize the SILC state,[10] making it possible to "turn-on" interlayer coherence in a system that exhibits no SILC at balance.[10,11] However, neither of these behaviors has been observed to date. Previous experiments have shown a parabolic increase in the stability with imbalance,[7–9] with no evidence for the turning-on of SILC with imbalance. In the present work, the removal of tunneling and the ability to alter the charge distribution over the entire range of imbalance has gone some way towards

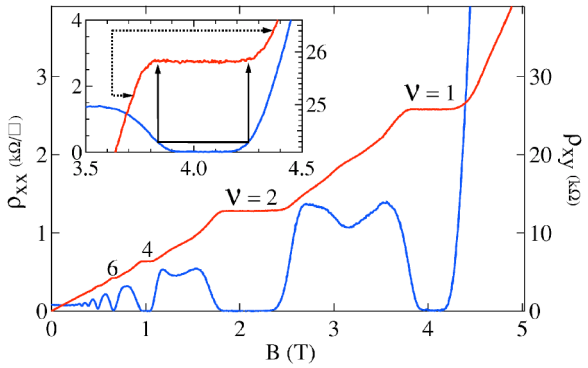

FIG. 1. Longitudinal $_{xx}$ and Hall $_{xy}$ resistivity traces obtained at balance ($n_t=n_b$) for $d/l_B=1.36$ ($n_T=9.7\times10^{10}$ cm^{-2}). The inset shows two equivalent methods of determining the width of the $\nu=1$ QH state based on $_{xy}$ (dashed) and $_{xx}$ (solid).

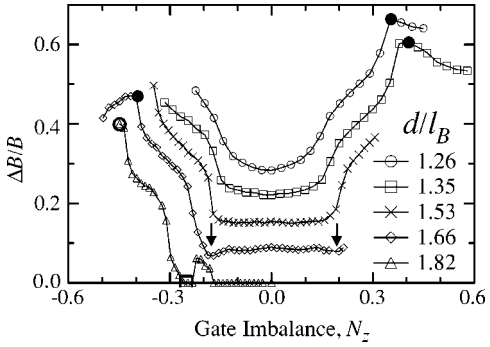

FIG. 2. Normalized width $\Delta B/B$ of the $\nu=1$ $_{xx}$ minima gate imbalance N_z for five d/l_B. The arrows indicate the composite $1/3+2/3$ states (see text) and the three solid and one open circles correspond to those shown in the simplified phase diagram (Fig. 3). Consecutive traces are offset by $\Delta B/B=0.04$ for clarity.

reconciling theory and experiment, and indicates that it is possible to turn on SILC with charge imbalance.

To overcome problems associated with tunneling, we have used a bilayer hole sample consisting of a (311) A GaAs/AlGaAs heterostructure with two 15 nm wide GaAs quantum wells separated by a 2.5 nm wide AlAs barrier. The larger effective mass of holes, compared to electrons, suppresses interlayer tunneling ($\Delta_{SAS}<0.1$ K). An *in situ* back gate allows a wide gate range so that we can achieve total charge imbalance. As an added advantage, bilayer hole systems allow measurements of devices with smaller d, and therefore larger n_T, where the effects of disorder are reduced.[6]

Electrical measurements were performed using standard low-frequency ac lock-in techniques with an excitation current $I<2$ nA at a lattice temperature of 55 mK. The two 2D hole layers are measured using a Hall bar geometry with ohmic contacts that contact both layers in parallel. The densities in the two layers are controlled electrostatically using gates above and below the 2D layers. Imbalance at constant n_T is achieved by adjusting the bias voltage on the top (V_t) and bottom (V_b) gates in opposite directions by amounts proportional to the respective gate-layer separation.[12]

Figure 1 shows longitudinal ($_{xx}$) and Hall ($_{xy}$) resistivities measured as a function of B at $d/l_B=1.36$ for the balanced bilayer system. The absence of QH states at odd integer ν 3 demonstrates that interlayer tunneling is negligible[5] and that the QH state at $\nu=1$ is entirely due to SILC.

The inset of Fig. 1 shows two equivalent methods of determining the stability of the SILC state by measuring its width in magnetic field. Sawada *et al.* have previously shown that the width of the $\nu=1$ quantum Hall plateau is a good measure of the QH state's activation energy obtained through thermal activation measurements.[7] This makes it experimentally possible to conveniently measure the stability of the SILC state as a function of both imbalance and total carrier density. In Ref. 7, the width of the QH plateau is obtained by measuring the range in magnetic field over which the Hall resistance was within $\pm2.5\%$ of h/e^2 (dashed arrows in the inset of Fig. 1) and subtracting the width of the classical Hall resistance over the same $\pm2.5\%$ range. However, the width of the SILC state can be determined more simply by measuring the range in magnetic field, ΔB, over which the longitudinal resistance is below a given cutoff $^c_{xx}$ (solid line in the inset of Fig. 1). This is because for $_{xy}$ to be quantized, $_{xx}$ must tend to zero.[1,3] We have checked that both the $_{xy}$ and $_{xx}$ methods of determining the stability of the SILC state are equivalent, with excellent qualitative agreement (and quantitative agreement to $\pm20\%$). To account for the dependence of the width of the quantum Hall state on the total carrier density n_T, we normalize ΔB to the magnetic field at which the quantum Hall state occurs ($\Delta B/B$). This is consistent with previous studies of single-layer QH systems,[13] which have shown that the normalized magnetic field width $\Delta B/B$ is a good measure of the activation gap.

Here we present data obtained from measurements of the width of the $_{xx}$ minimum, since these same data can also be used to determine the carrier density in each layer and follow the evolution of other QH states through the low field $_{xx}$ oscillations. This additional information will be essential for interpreting several features of the evolution of the SILC state under charge imbalance, as discussed below.

To quantify the charge imbalance, we introduce two parameters—the layer imbalance m_z and the gate imbalance N_z. The layer imbalance $m_z=(n_t-n_b)/n_T$ is also known as the z component of the pseudospin vector,[4] and describes the fractional charge imbalance between the two layers. The layer imbalance takes values of $m_z=+1$, 0, and -1 when all holes are in the top layer, equally balanced, and in the bottom layer, respectively. The gate imbalance is the analog of m_z for the top and bottom gates, and describes the fraction of charge moved from one gate to another: $N_z=(\Delta N_t-\Delta N_b)/N_T$, where $N_T=N_t+N_b$ is the total surface charge on the gates, $\Delta N_{t,b}$ $V_{t,b}/d_{t,b}$ is the change in the top or bottom gate surface charge density from its value at balance, and $V_{t,b}$ is the bias applied to the top/bottom layer, assuming $V_{t,b}=0$ V at balance. The distance $d_{t,b}$ is the gate-layer separation for the top/bottom layer. For a classical system, the gate and layer imbalances are equal, $N_z=m_z$. However, in our bilayer 2D hole systems, $|m_z|$ $|N_z|$, due to the strong negative compressibility caused by exchange-correlation effects.[6,10]

Figure 2 shows measurements of the stability $\Delta B/B$ of the

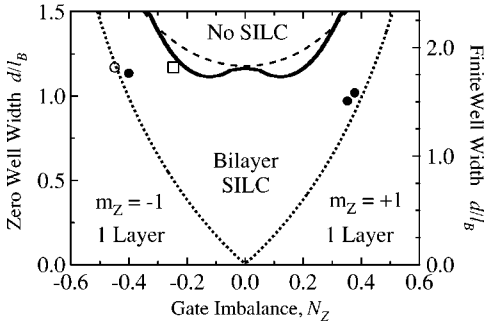

FIG. 3. Simplified ground-state phase diagram for this bilayer $\nu=1$ system. Solid and dashed lines mark the boundary between SILC and non-SILC states with and without intralayer correlations, respectively. Dotted line indicates the transition between bilayer and single-layer charge distributions. The symbols correspond to the data points highlighted in Fig. 2.

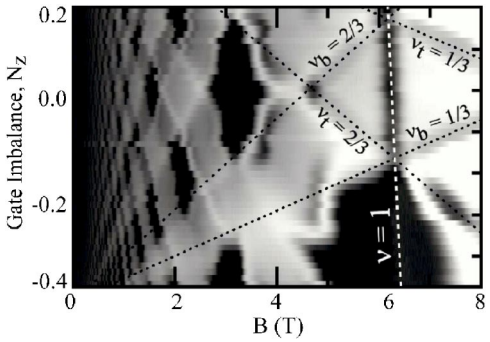

FIG. 4. Grey-scale plot of $_{xx}$ (z axis) B and N_z. Dark regions correspond to QH states. The four diagonal dotted lines denote single-layer fractional QH states and the vertical white dotted line follows the bilayer $\nu=1$ QH state.

bilayer $\nu=1$ QH state obtained as a function of gate imbalance N_z for five different values of d/l_B ranging from 1.26 (top) to 1.82 (bottom). Our three key results are evident in this data, which we discuss in order of increasing d/l_B. Commencing with the lowest d/l_B (top trace), we observe an approximately parabolic increase in $\Delta B/B$ with increasing N_z for small imbalance $|N_z|<0.15$, consistent with Refs. 7 and 9. However, as d/l_B is increased to 1.53 (middle trace in Fig. 3) the parabola acquires a flat bottom, as expected from Hartree-Fock calculations.[11] It is unclear why this behavior has not been observed in previous experiments,[7–9] and why the predicted behavior is only observed at larger d/l_B, since the Hartree-Fock calculations should improve as $d/l_B \to 0$. One possibility is that topological excitations[4] (not considered in Ref. 11) cause deviations from the Hartree-Fock predictions at smaller d/l_B. A second possibility is that since smaller d/l_B requires low n_T, disorder may play a role.

Our first key result is that for $|N_z|>0.2$ all the d/l_B traces evolve similarly—$\Delta B/B$ rises sharply towards a clear peak and then decreases gradually with increasing imbalance. These $\Delta B/B$ peaks are marked with solid circles for the $d/l_B=1.26$, 1.35, and 1.66 traces in Fig. 2, and these data points are also mapped onto Fig. 3 with the same symbols. For $d/l_B=1.82$ we were unable to resolve the precise location of the peak (because the $\nu=1$ state extended beyond the maximum B of the measurements at large imbalance), but the data shows that it occurs for $|N_z|$ 0.45, indicated by the open circle.

Figure 3 introduces a simplified phase diagram for the existence of the SILC state in our bilayer system calculated as a function of N_z and d/l_B. The left y axis shows the theoretical d/l_B and the right y axis shows the equivalent d/l_B after accounting for finite well thickness.[14] The SILC state is unstable above the dashed line according to the calculations of Refs. 10 and 11. The solid line shows the same phase boundary after intralayer correlations have been considered (i.e., comparing the ground-state energy of the SILC state with those of two independent single-layer states[15]). The thin dotted line marks the calculated point at which the gate imbalance drives all the charge into one layer, corresponding to $m_z=\pm 1$ (exchange and correlation effects cause this to occur for $|N_z|<1$).

Mapping the circles from the experimental data in Fig. 2 onto the phase diagram in Fig. 3, we find that the measured peaks in $\Delta B/B$ in Fig. 2 correspond to the points at which total charge transfer is predicted to occur. This indicates that the peak in $\Delta B/B$ is a signature of the transition from a bilayer to a single-layer charge distribution at $\nu=1$. This transition occurs at $|N_z|<1$ due to exchange-correlation effects. We also note that the N_z where total charge transfer occurs decreases with decreasing density, consistent with the dotted line in Fig. 2. We note that a similar sharp change in the width of the $\nu=1$ state was also seen in bilayer systems with increasing imbalance when the charge density was not kept constant,[6] but this was not commented on.

Our second key result comes from the $d/l_B=1.66$ trace in Fig. 2. At $d/l_B=1.66$, the interlayer correlations are weak and therefore the SILC state is susceptible to perturbations from intralayer correlations. The downward pointing arrows in Fig. 2 mark the point at which $\nu_t=1/3$ and $\nu_b=2/3$ (left), and $\nu_t=2/3$ and $\nu_b=1/3$ (right), for the $d/l_B=1.66$ trace. These are the points at which single-layer fractional QH states generate the strongest intralayer correlations. The single-layer fractional QH states coincide with measured minima in the stability of the SILC state. This suggests that the minima in the stability of the SILC state are the result of the composite $\nu=1/3+2/3$ intralayer correlated state competing with interlayer correlated SILC state: Changing the imbalance alters the energy of the composite state with respect to the SILC state, so that at $|N_z|=0.18$ the gap between the two is minimized, reducing the activation energy (and hence ΔB) of the SILC state.

To confirm that competition between the SILC state and the combined $1/3+2/3$ state is responsible for this effect, we track the evolution of the SILC $\nu=1$ state and four single-layer fractional QH states in Fig. 4. The grey-scale plot in Fig. 4 consists of 36 separate traces of $_{xx}$ (z axis) versus B (x axis) obtained at different values of N_z (y axis). The dark regions correspond to $_{xx}$ minima (i.e., QH states). We have labeled five significant QH states in this plot: The diagonal black dashed lines indicate the four single-layer fractional QH states: $\nu_t=\frac{1}{3}$, $\nu_b=\frac{1}{3}$, $\nu_t=\frac{2}{3}$, and $\nu_b=\frac{2}{3}$. The light near-vertical dashed line marks the magnetic field at which $\nu=1$. In the data the bilayer $\nu=1$ state is manifested as a vertical dark band centered on this vertical line, bounded by the four

diagonal lines. Most significantly, the $\nu=1$ state is weakest at $N_z=\pm 0.18$ where it intersects the diagonal lines that mark the single layer $\nu=1/3$ and $\nu=2/3$ states. The weakening of the $\nu=1$ bilayer QH state is indicated on the grayscale by a significantly lighter shade of gray at these N_z. These two gray regions correspond to the local minima in the $d/l_B=1.66$ trace in Fig. 2, and directly reveal the competition between the SILC state and the composite $\frac{1}{3}+\frac{2}{3}$ independent layer state at $\nu=1$. This competition between the SILC state and the composite state is not observed at smaller d/l_B because the interlayer coherence becomes stronger and intralayer correlations become weaker as d/l_B decreased (i.e., as l_B increases).

Finally, and most importantly, we find that a bilayer system that is incoherent at balance can develop SILC with charge imbalance in agreement with Ref. 11. Increasing d/l_B to 1.82 (lowest trace in Fig. 2) destroys the SILC state at $N_z=0$ ($\Delta B/B\rightarrow 0$), and the system behaves as two independent layers. As the layers are then imbalanced, proceeding left from the center in the $d/l_B=1.82$ trace in Fig. 2, there is initially no QH state at $\nu=1$ until N_z reaches -0.2, where a well-defined peak in $\Delta B/B$ (as opposed to the minimum at $d/l_B=1.66$) indicates the formation of a composite $\nu=1$ states with $\nu_t=\frac{1}{3}$ and $\nu_b=\frac{2}{3}$ (i.e., this state has no SILC but strong intralayer correlations). This is verified using a greyscale plot similar to Fig. 4 (not shown). A small increase in imbalance to $N_z=-0.23$ destroys the composite state (i.e., $\Delta B/B$ returns to zero, highlighted by the open square in Fig. 2). Upon further imbalance, $\Delta B/B$ again becomes nonzero and begins to rise rapidly out to $N_z=-0.45$ (the limit of the experimental data, indicated by the open circle in Fig. 2). To understand the origins of this sharp rise in the stability of $\nu=1$ beyond $N_z=-0.23$, we map the points at which the rise starts and stops onto the phase diagram in Fig. 3, using open symbols. The open square lies on the boundary between the "no SILC" phase and the SILC phase, and the open circle lies on the $m_z=\pm 1$ boundary. This suggests that the onset of the steep rise in $\Delta B/B$ corresponds to turning-on interlayer coherence with charge imbalance, and the peak in $\Delta B/B$ occurs when all the charge has transferred into one layer ($m_z=\pm 1$). We note that the same steep rise in $\Delta B/B$ occurs for all values of d/l_B once the imbalance exceeds some critical value $|N_z|$, whether or not a $\nu=1$ QH state exists at $N_z=0$.

In conclusion, we used low-density, high-mobility bilayer hole systems with negligible tunneling to map the stability of the bilayer $\nu=1$ QH state versus charge imbalance at constant total density for five values of d/l_B ranging from strongly interlayer coherent ($d/l_B=1.26$) to incoherent ($d/l_B=1.82$) at balance. We observe three key results: (i) the significant enhancement of total charge transfer due to exchange-correlation effects, (ii) the presence of direct competition between the SILC state and composite single-layer fractional QH state in weakly coherent systems, and most significantly that (iii) bilayer systems that are incoherent at balance develop spontaneous interlayer coherence with imbalance. We note that as $|m_z|\rightarrow 1$, the pseudospin stiffness[4] tends to zero, making SILC susceptible to destruction by disorder and quantum fluctuations. Recently, work subsequent to ours has appeared that also investigates the effect of charge imbalance on SILC.[16]

This work was supported by the Australian Research Council, by NSF Grant Nos. DMR-0206681 and EPS-0132626, and by a grant from the Research Corporation.

*Email address: wclarke@phys.unsw.edu.au

[1] K. von Klitzing, G. Dorda, and M. Pepper, Phys. Rev. Lett. **45**, 494 (1980).

[2] D. C. Tsui, H. L. Störmer, and A. C. Gossard, Phys. Rev. Lett. **48**, 1559 (1982).

[3] J. P. Eisenstein, *Perspectives in Quantum Hall Effects*, edited by S. Das Sarma and A. Pinczuk (Wiley, New York, 1997), Chaps. 1 and 2.

[4] S. M. Girvin and A. H. MacDonald, *Perspectives in Quantum Hall Effects*, Ref. 3, Chap. 5; S. M. Girvin, Phys. Today **53** (6), 39 (2000).

[5] G. S. Boebinger, H. W. Jiang, L. N. Pfeiffer, and K. W. West, Phys. Rev. Lett. **64**, 1793 (1990).

[6] A. R. Hamilton, M. Y. Simmons, F. M. Bolton, N. K. Patel, I. S. Millard, J. T. Nicholls, D. A. Ritchie, and M. Pepper, Phys. Rev. B **54**, R5259 (1996).

[7] A. Sawada, Z. F. Ezawa, H. Ohno, Y. Horikoshi, Y. Ohno, S. Kishimoto, F. Matsukura, M. Yasumoto, and A. Urayama, Phys. Rev. Lett. **80**, 4534 (1998).

[8] V. T. Dolgopolov, A. A. Shashkin, E. V. Deviatov, F. Hastreiter, M. Hartung, A. Wixforth, K. L. Campman, and A. C. Gossard, Phys. Rev. B **59**, 13 235 (1999).

[9] E. Tutuc, S. Melinte, E. P. De Poortere, R. Pillarisetty, and M. Shayegan, Phys. Rev. Lett. **91**, 076802 (2003).

[10] C. B. Hanna, Bull. Am. Phys. Soc. **42** (1), 553 (1997).

[11] Y. N. Joglekar and A. H. MacDonald, Phys. Rev. B **65**, 235319 (2002).

[12] C. B. Hanna, D. Haas, and J. C. Díaz-Vélez, Phys. Rev. B **61**, 13 882 (2002).

[13] F. Y. Huang, Phys. Lett. A **294**, 117 (2002).

[14] S. He, S. Das Sarma, and X. C. Xie, Phys. Rev. B **47**, 4394 (1993).

[15] Single-layer ground-state energies provided by A. H. MacDonald (private communication).

[16] I. B. Spielman, M. Kellogg, J. P. Eisenstein, L. N. Pfeifer, and K. W. West, Phys. Rev. B **70**, 081303 (2004); R. D. Wiersma, J. G. S. Lok, S. Kraus, W. Dietsche, K. von Klitzing, D. Schuh, M. Bichler, H. P. Tranitz, and W. Wegscheider, cond-mat/0407591 (unpublished).